

# Supplementary Materials: NHI and NHC-Supported Al(III) Hydrides for Amine–Borane Dehydrocoupling Catalysis

Catherine Weetman, Nozomi Ito, Masafumi Unno, Franziska Hanusch and Shigeyoshi Inoue \*

## Contents

1. Catalysis.....	1
2. Mechanistic Studies.....	8
2.1. NHI Mechanism .....	8
3. Data for compounds <b>8</b> <sup>iPr</sup> and <b>9</b> .....	12
3.1 Compound <b>8</b> <sup>iPr</sup> .....	12
3.2 Compound <b>9</b> .....	14
4. X-ray Data .....	15

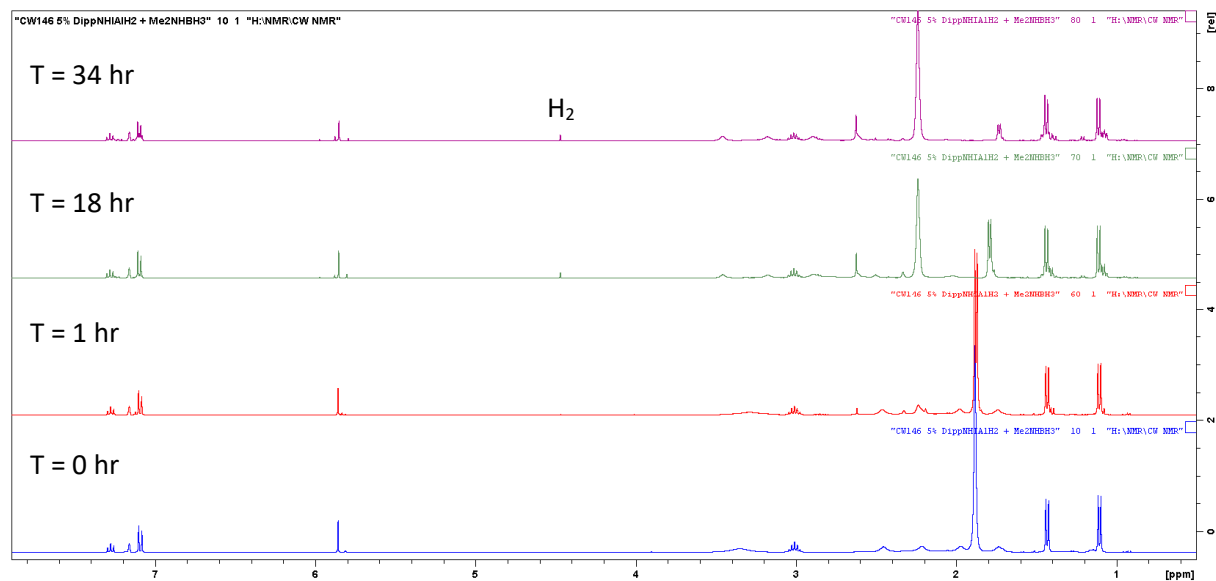
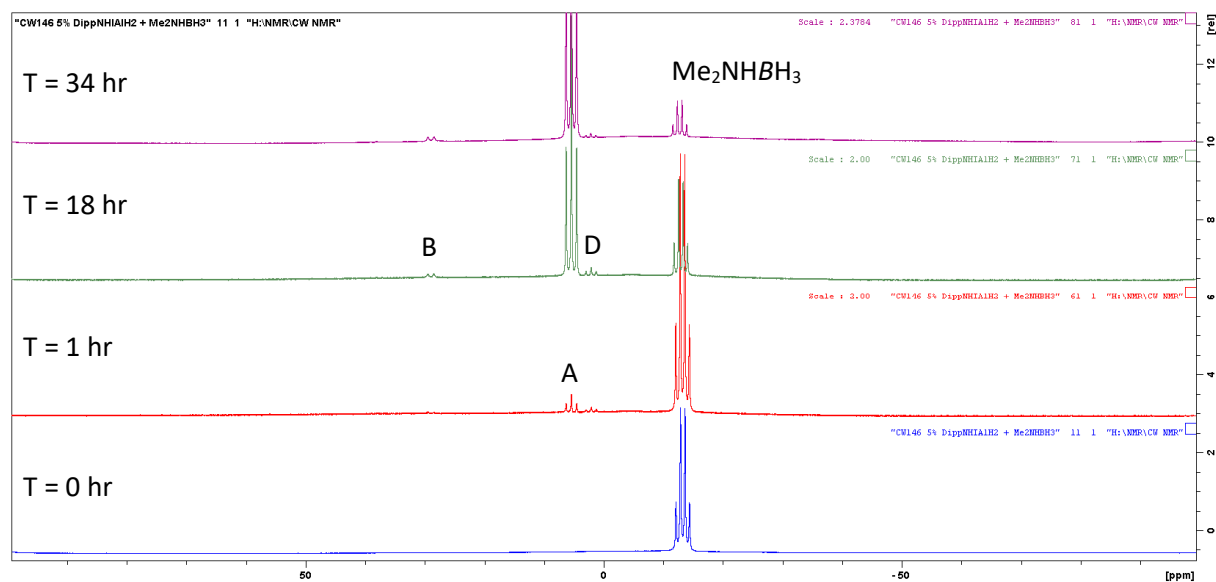
## 1. Catalysis

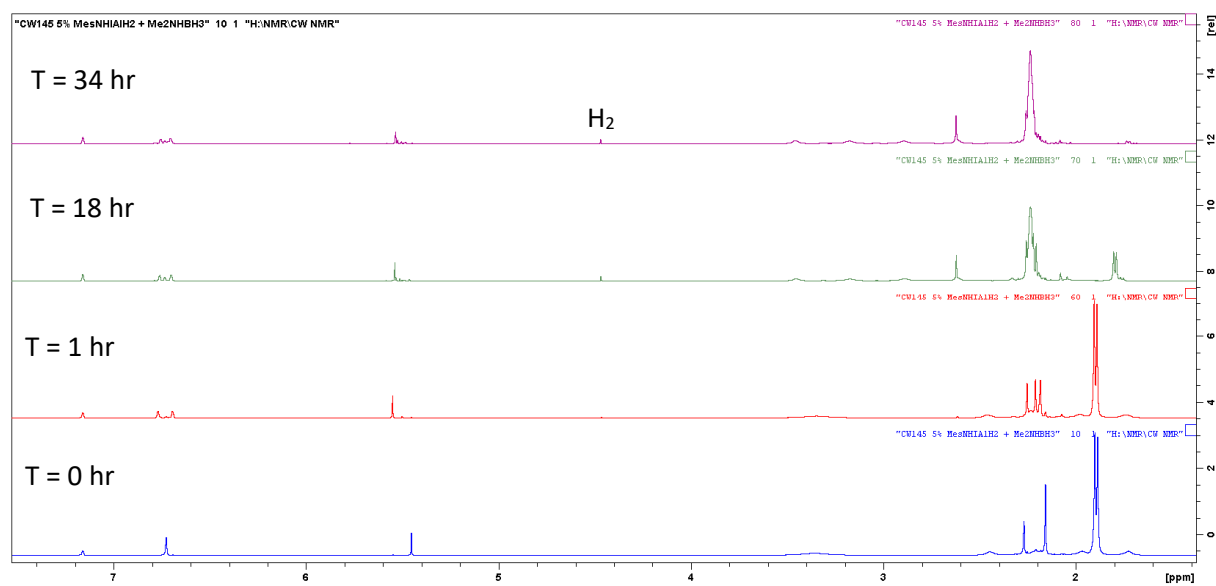
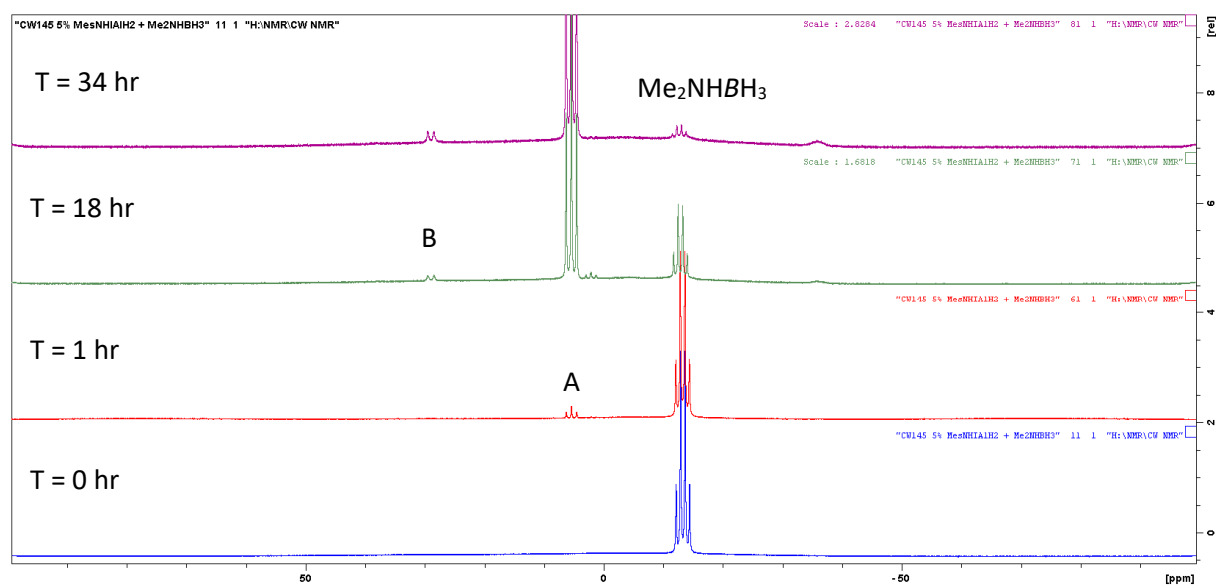
*General procedure:* 5 mol% of chosen catalyst (**1-6**, 0.012 mmol) and Me<sub>2</sub>NHBH<sub>3</sub> (0.24 mmol) were dissolved in 0.5 mL of C<sub>6</sub>D<sub>6</sub> and added to a Youngs Tap NMR tube. <sup>1</sup>H and <sup>11</sup>B NMR was recorded before being placed at the appropriate temperature and monitored over time until >80% consumption of Me<sub>2</sub>NHBH<sub>3</sub>.

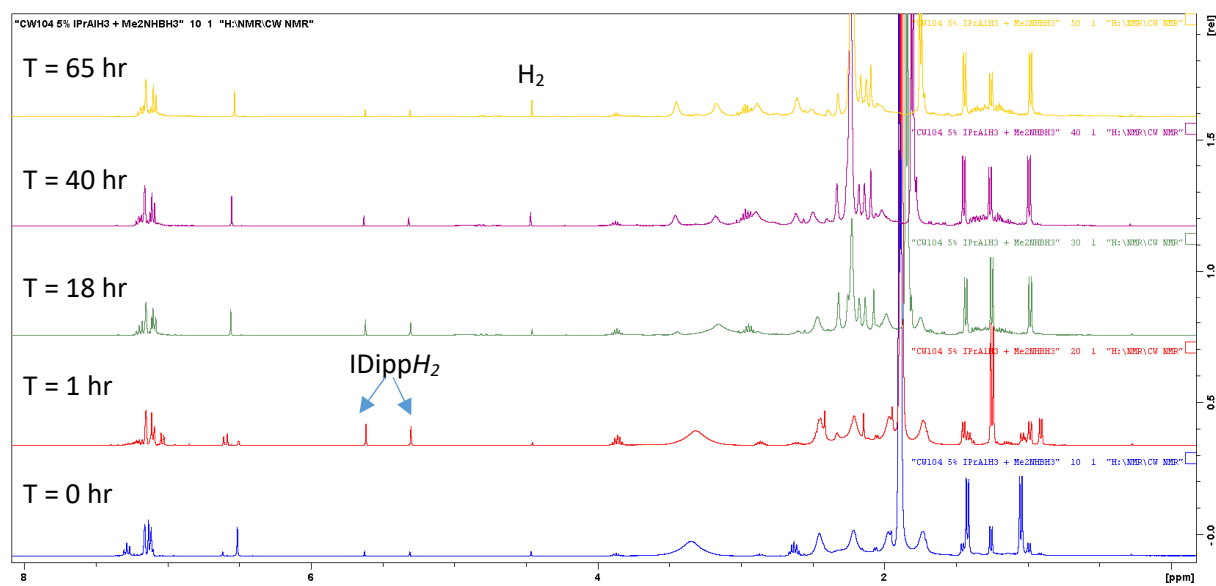
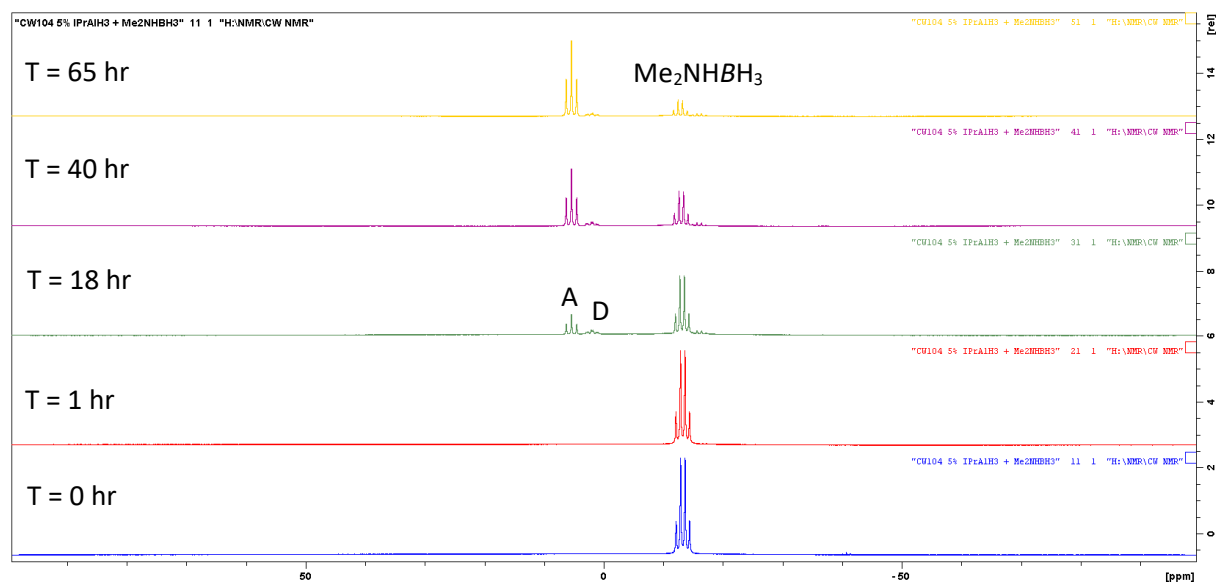
Table S 1. Dehydrocoupling of Me<sub>2</sub>NHBH<sub>3</sub> with 5 mol% Al(II) hydride catalysts **1-6**

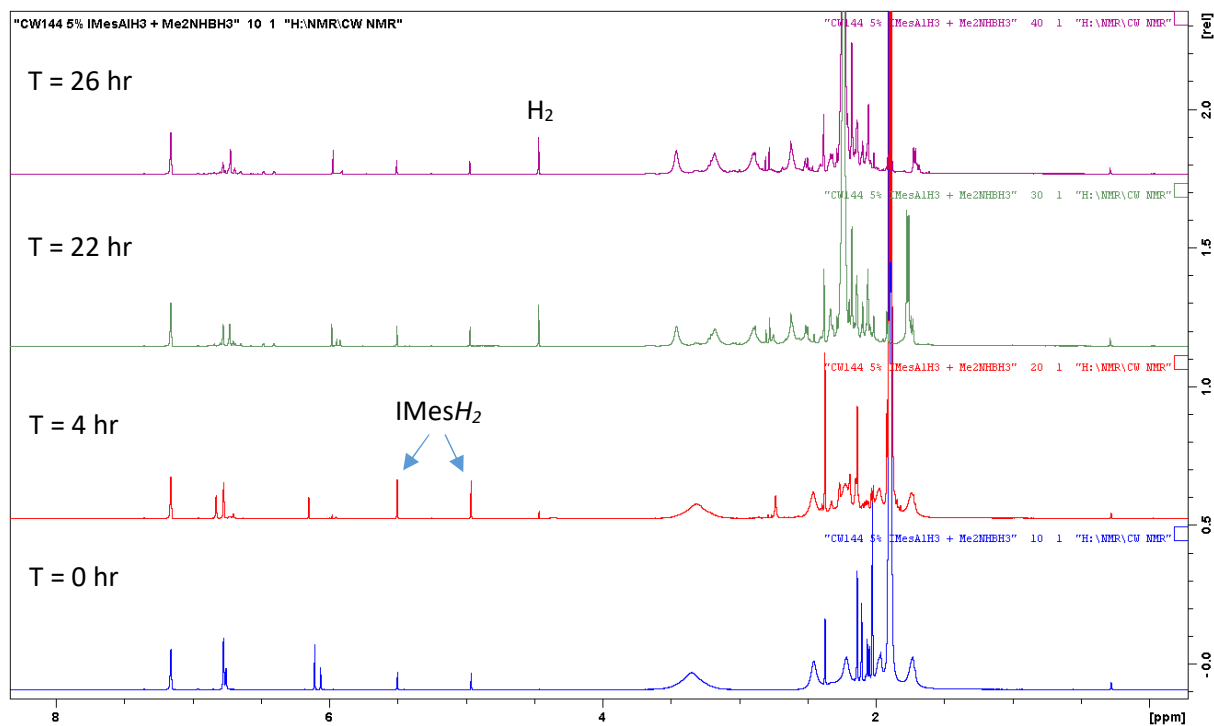
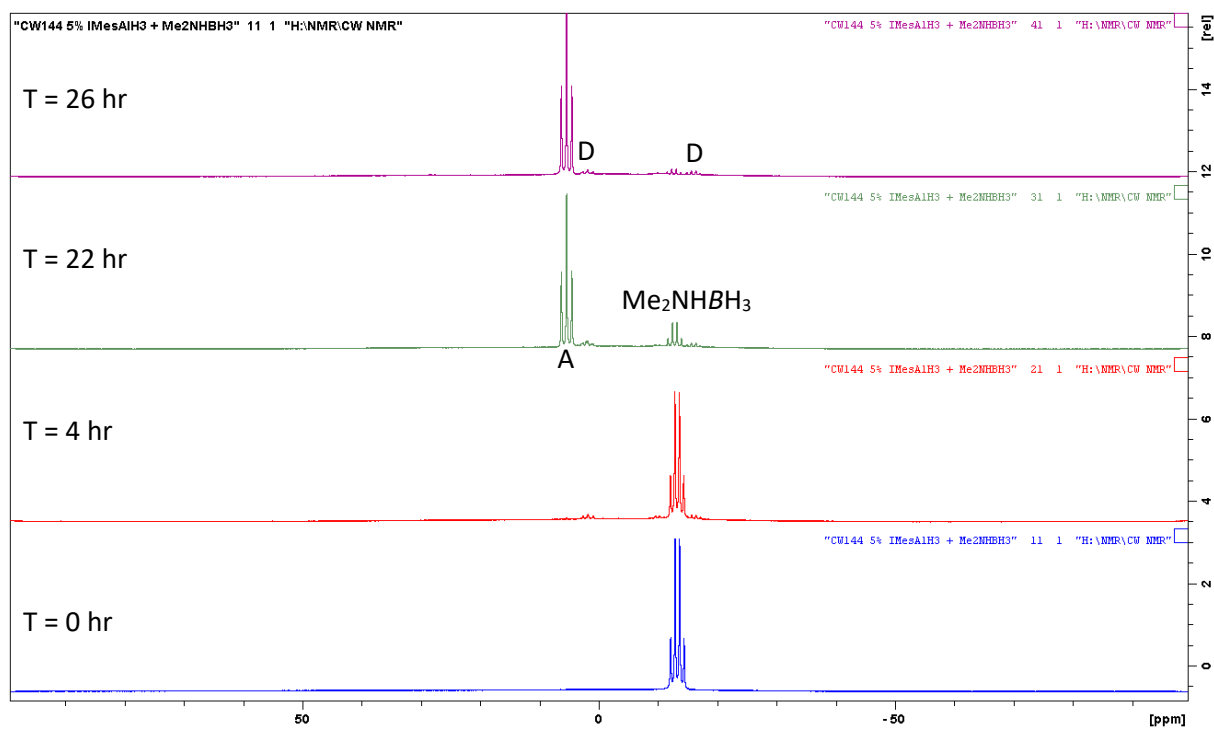
Catalyst	Temp/ °C	Time/ hr	Conversion <sup>a</sup> / %	TOF <sup>b</sup> / hr <sup>-1</sup>	Product distribution				
					A	B	C	D	Others
<b>1</b>	80	34	90	0.53	76	2	-	6	-
<b>2</b>	80	34	84	0.49	85	5	-	-	-
<b>3</b>	50	65	80	0.25	70	-	-	6	4
<b>4</b>	50	26	92	0.74	76	-	-	9	7
<b>5</b>	50	65	93	0.29	66	-	-	9	18
<b>6</b>	50	40	92	0.46	72	-	-	8	15

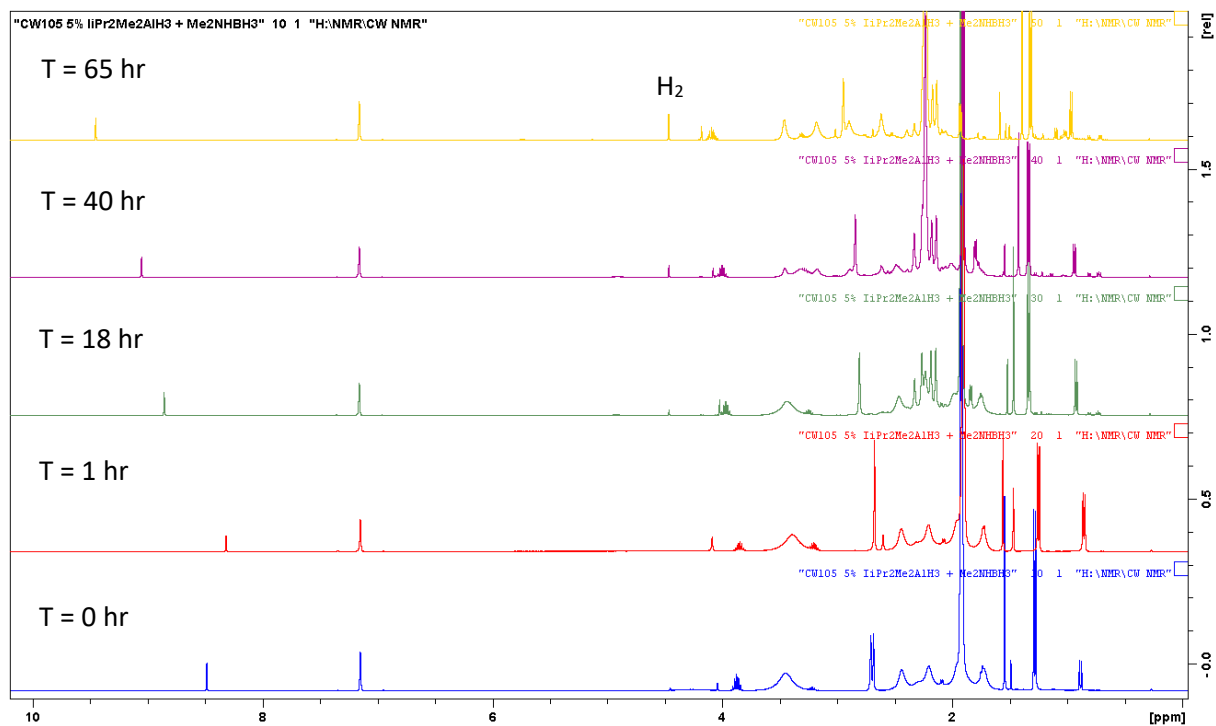
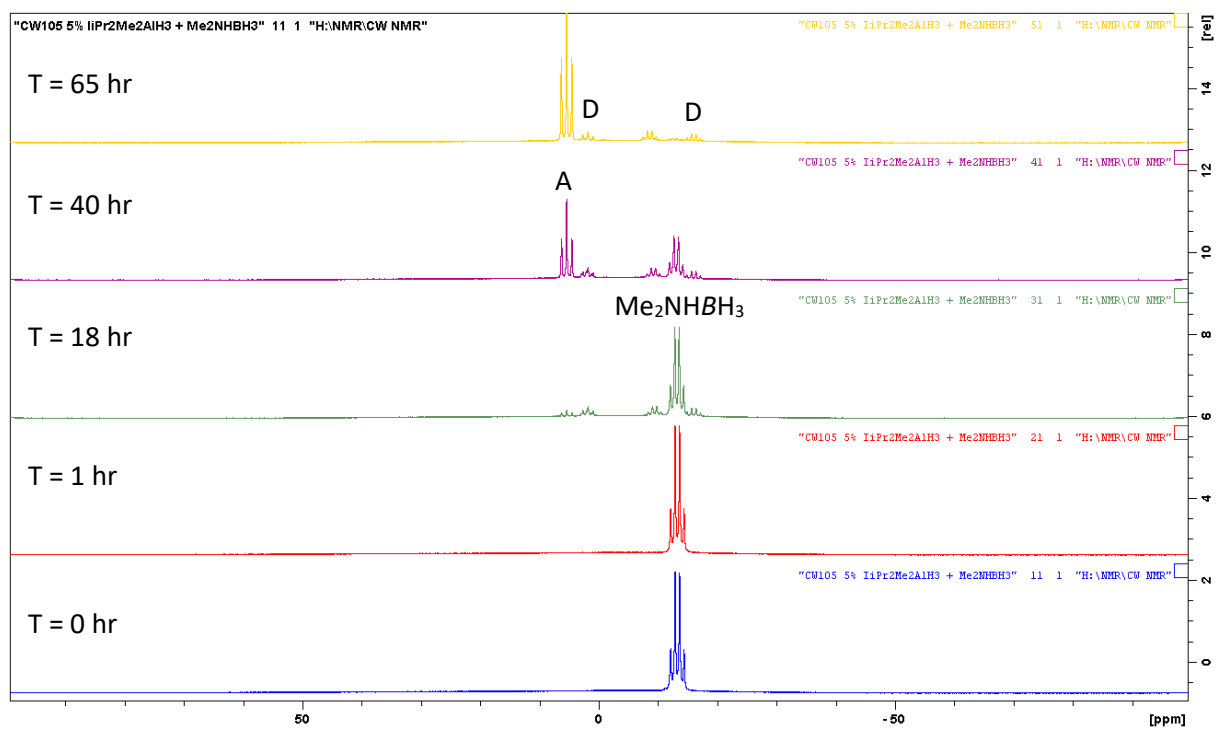
Reaction conditions 5 mol% **1-6** (0.012 mmol), Me<sub>2</sub>NHBH<sub>3</sub> (0.24 mmol), 0.5 mL C<sub>6</sub>D<sub>6</sub>. <sup>a</sup> conversion of Me<sub>2</sub>NHBH<sub>3</sub> determined by <sup>11</sup>B NMR relative integrals; <sup>b</sup> TOF = (conversion/catalyst loading)/time

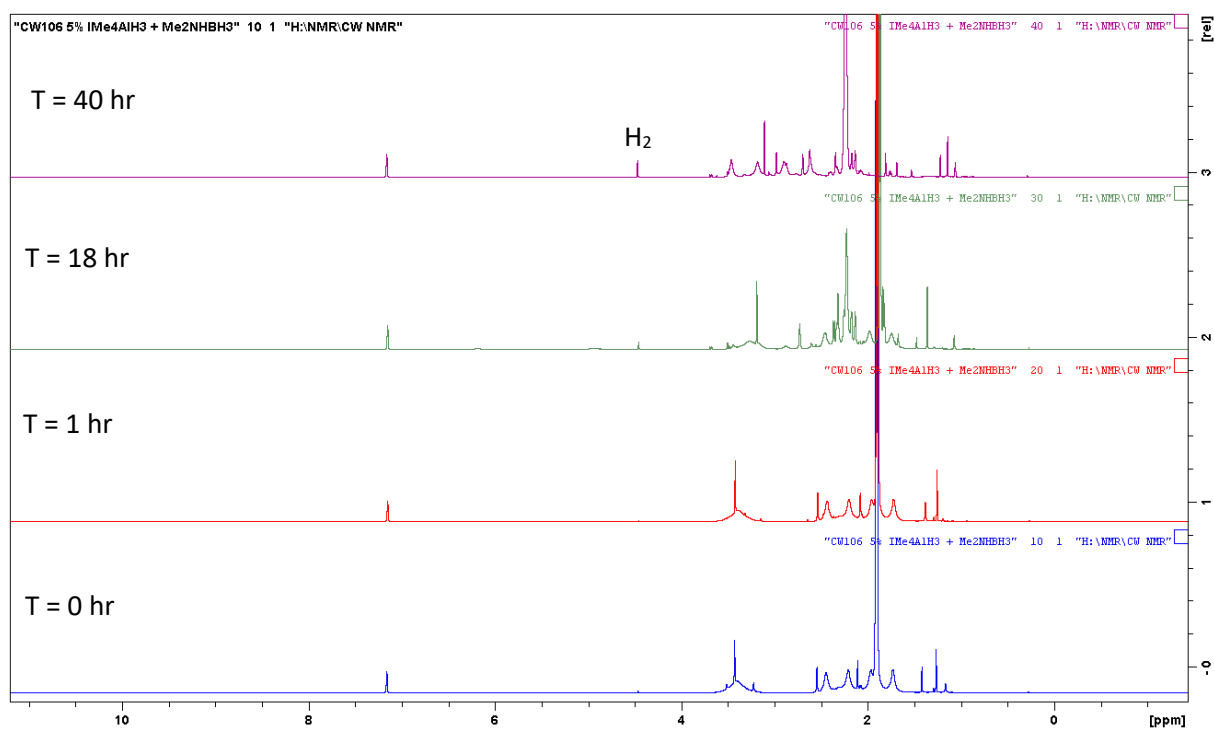
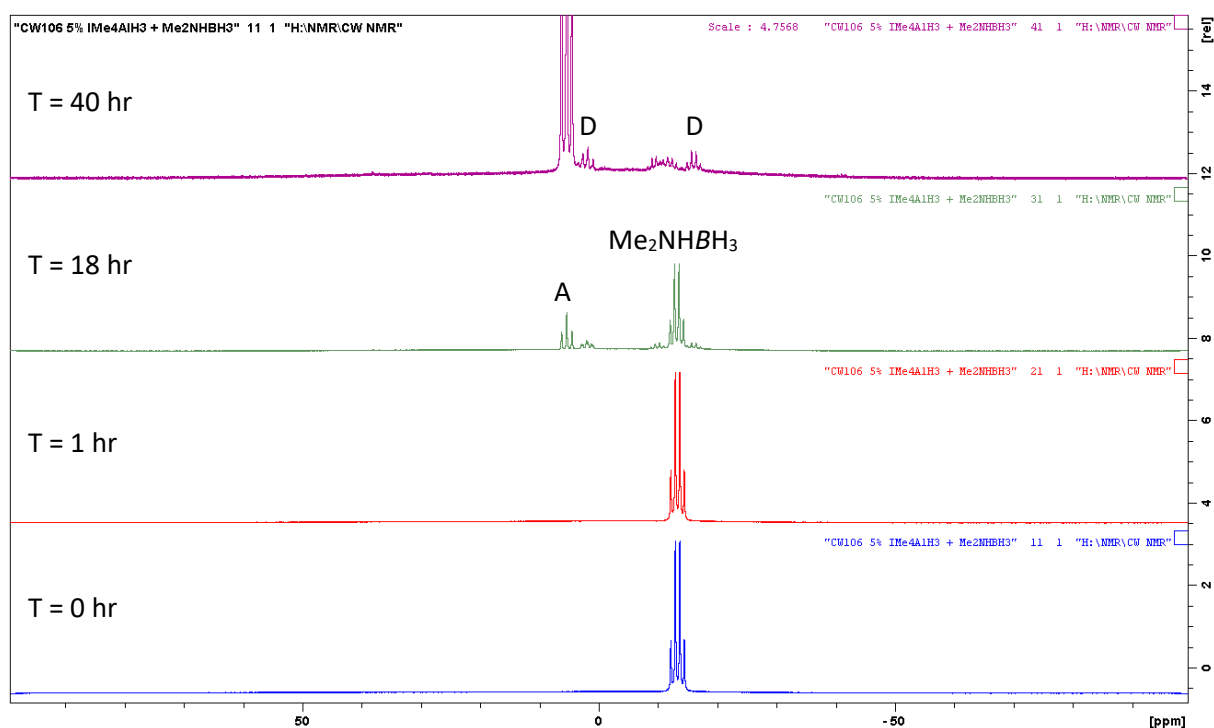
Figure S 1. Stacked  $^1\text{H}$  NMR spectra for 5 mol% 1 with  $\text{Me}_2\text{NBH}_3$  at  $80^\circ\text{C}$  in  $\text{C}_6\text{D}_6$ Figure S 2. Stacked  $^{11}\text{B}$  NMR spectra for 5 mol% 1 with  $\text{Me}_2\text{NBH}_3$  at  $80^\circ\text{C}$  in  $\text{C}_6\text{D}_6$

Figure S 3. Stacked  $^1\text{H}$  NMR spectra for 5 mol% **2** with  $\text{Me}_2\text{NBH}_3$  at  $80^\circ\text{C}$  in  $\text{C}_6\text{D}_6$ Figure S 4. Stacked  $^{11}\text{B}$  NMR spectra for 5 mol% **2** with  $\text{Me}_2\text{NBH}_3$  at  $80^\circ\text{C}$  in  $\text{C}_6\text{D}_6$

Figure S 5. Stacked  $^1\text{H}$  NMR spectra for 5 mol% **3** with  $\text{Me}_2\text{NBH}_3$  at  $50^\circ\text{C}$  in  $\text{C}_6\text{D}_6$ Figure S 6. Stacked  $^{11}\text{B}$  NMR spectra for 5 mol% **3** with  $\text{Me}_2\text{NBH}_3$  at  $50^\circ\text{C}$  in  $\text{C}_6\text{D}_6$

Figure S 7. Stacked  $^1\text{H}$  NMR spectra for 5 mol% **4** with  $\text{Me}_2\text{NBH}_3$  at  $50^\circ\text{C}$  in  $\text{C}_6\text{D}_6$ Figure S 8. Stacked  $^{11}\text{B}$  NMR spectra for 5 mol% **4** with  $\text{Me}_2\text{NBH}_3$  at  $50^\circ\text{C}$  in  $\text{C}_6\text{D}_6$

Figure S 9. Stacked  $^1\text{H}$  NMR spectra for 5 mol% 5 with  $\text{Me}_2\text{NBH}_3$  at  $50^\circ\text{C}$  in  $\text{C}_6\text{D}_6$ Figure S 10. Stacked  $^{11}\text{B}$  NMR spectra for 5 mol% 5 with  $\text{Me}_2\text{NBH}_3$  at  $50^\circ\text{C}$  in  $\text{C}_6\text{D}_6$

Figure S 11. Stacked  $^1\text{H}$  NMR spectra for 5 mol% **6** with  $\text{Me}_2\text{NBH}_3$  at  $50^\circ\text{C}$  in  $\text{C}_6\text{D}_6$ Figure S 12. Stacked  $^{11}\text{B}$  NMR spectra for 5 mol% **6** with  $\text{Me}_2\text{NBH}_3$  at  $50^\circ\text{C}$  in  $\text{C}_6\text{D}_6$

## 2. Mechanistic Studies

### 2.1. NHI Mechanism

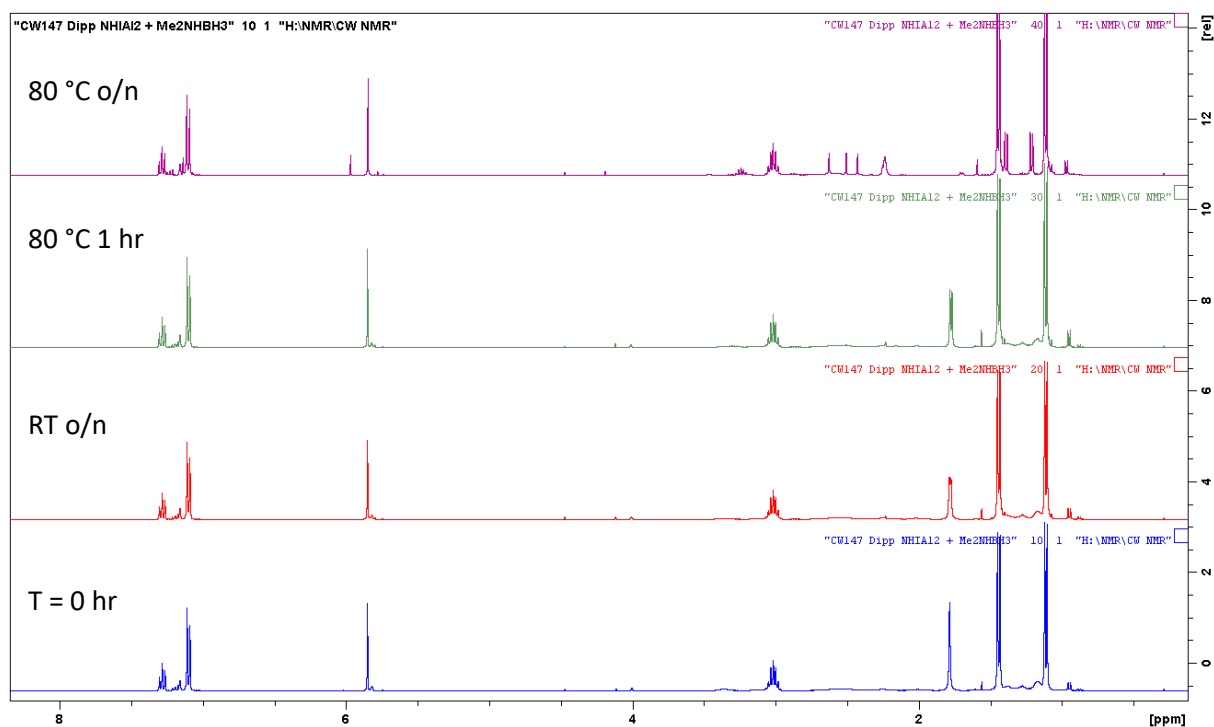


Figure S 13. Stacked  $^1\text{H}$  NMR spectra for stoichiometric reaction between **1** and  $\text{Me}_2\text{NHBH}_3$  in  $\text{C}_6\text{D}_6$ . No reaction occurred at room temperature. At 80 °C o/n resulted in consumption of  $\text{Me}_2\text{NHBH}_3$  with minor formation of compound **7**.

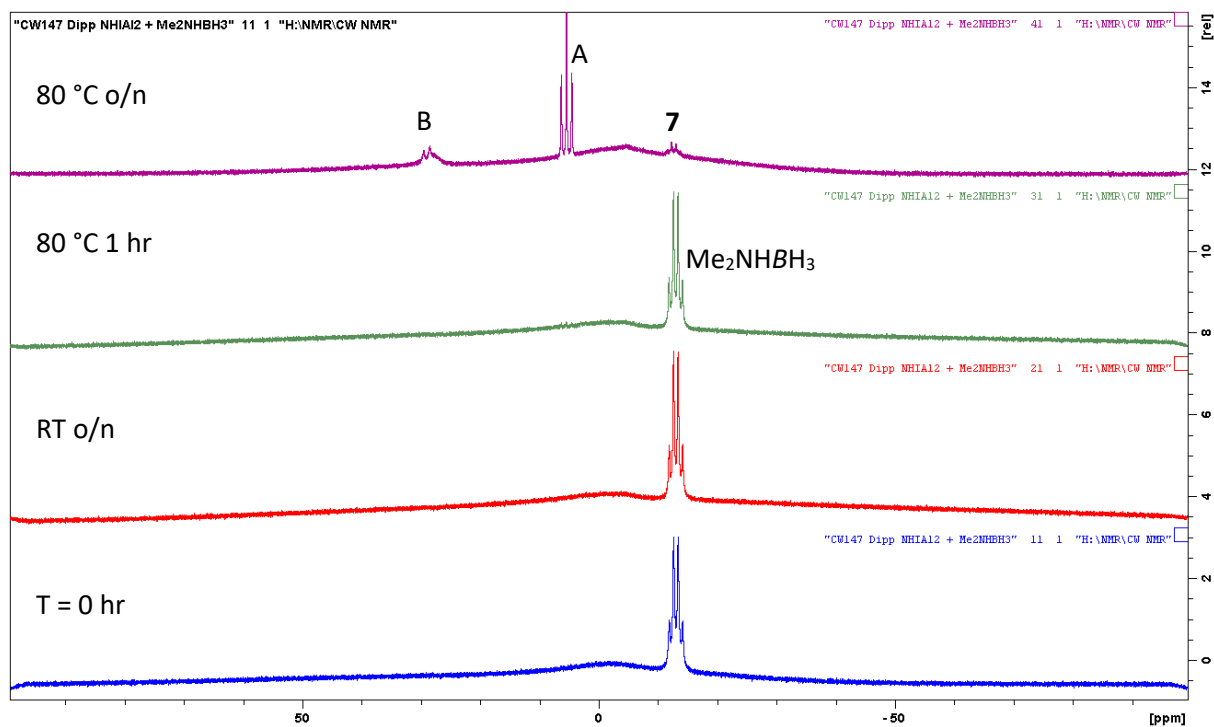


Figure S 14. Stacked  $^{11}\text{B}$  NMR spectra for stoichiometric reaction between **1** and  $\text{Me}_2\text{NHBH}_3$  in  $\text{C}_6\text{D}_6$ . No reaction occurred at room temperature. At 80 °C o/n resulted in consumption of  $\text{Me}_2\text{NHBH}_3$  with minor formation of compound **7**.

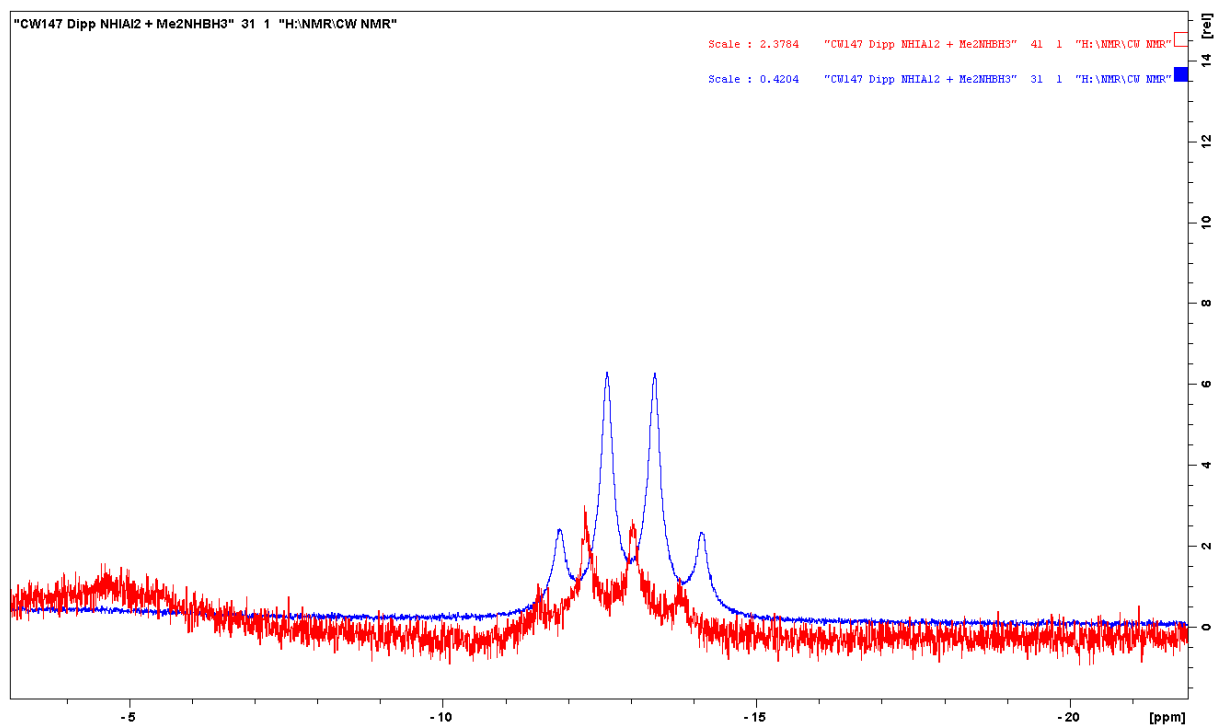


Figure S 15. Overlay of  $^{11}\text{B}$  spectra depicting minor shift in consumption of  $\text{Me}_2\text{NHBH}_3$  (blue spectrum) to formation of compound **7** (red spectrum).

## 2.2. NHC Mechanism

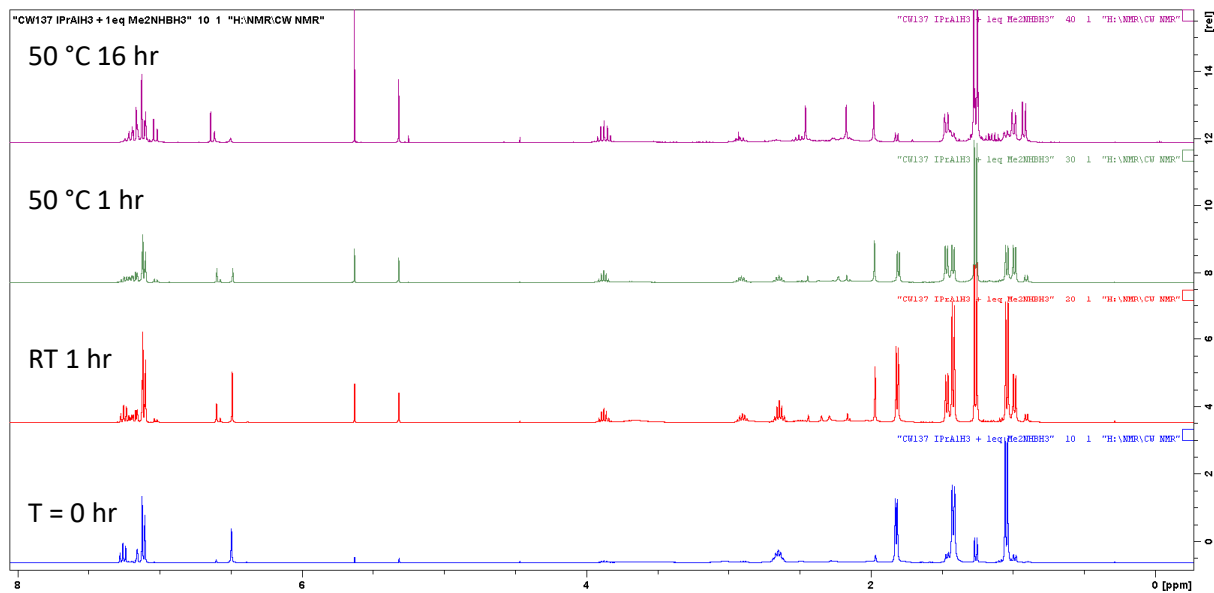


Figure S 16. Stacked  $^1\text{H}$  NMR spectra for stoichiometric reaction between **3** and  $\text{Me}_2\text{NHBH}_3$  in  $\text{C}_6\text{D}_6$ . No reaction occurred at room temperature. At  $50\text{ }^\circ\text{C}$  o/n resulted in consumption of  $\text{Me}_2\text{NHBH}_3$  with formation of compound **9**.

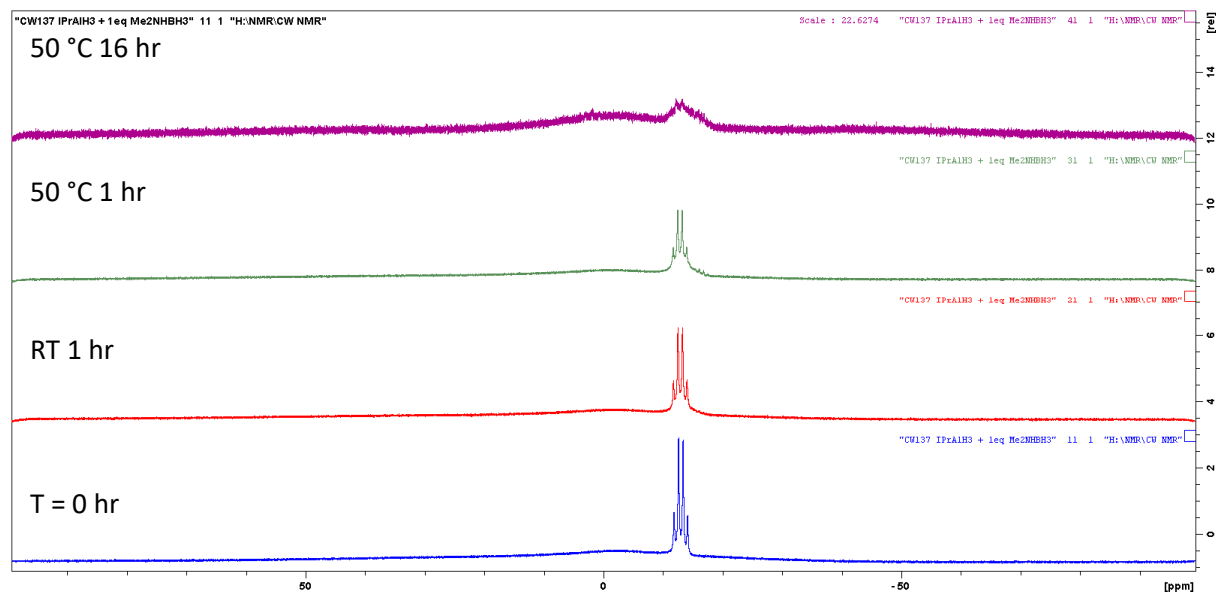


Figure S 17. Stacked  $^{11}\text{B}$  NMR spectra for stoichiometric reaction between **3** and  $\text{Me}_2\text{NHBH}_3$  in  $\text{C}_6\text{D}_6$ . No reaction occurred at room temperature. At  $50\text{ }^\circ\text{C}$  o/n resulted in consumption of  $\text{Me}_2\text{NHBH}_3$  with formation of compound **9**.

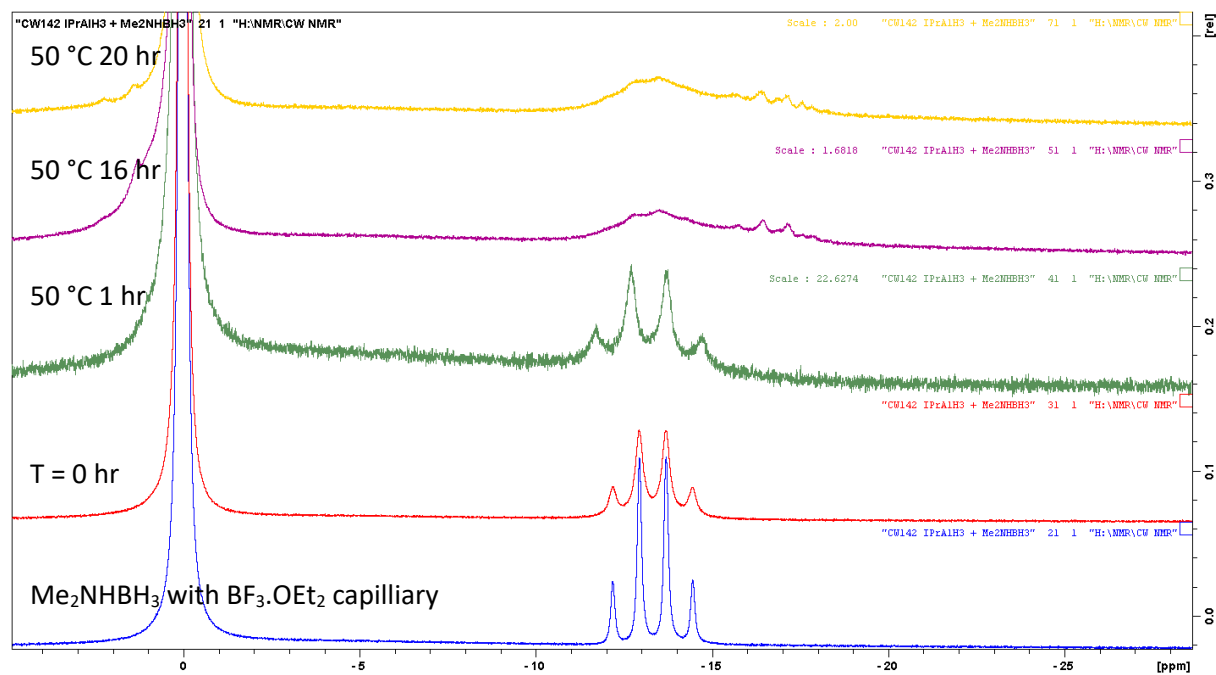


Figure S 18. Stacked  $^{11}\text{B}$  NMR spectra (0 to -25 ppm, with  $\text{BF}_3\cdot\text{OEt}_2$ ) for stoichiometric reaction between **3** and  $\text{Me}_2\text{NHBH}_3$  in  $\text{C}_6\text{D}_6$ . No reaction occurred at room temperature.  $50\text{ }^\circ\text{C}$  1hr resulted in formation of compound **8** additional heating resulted formation of compound **9**.

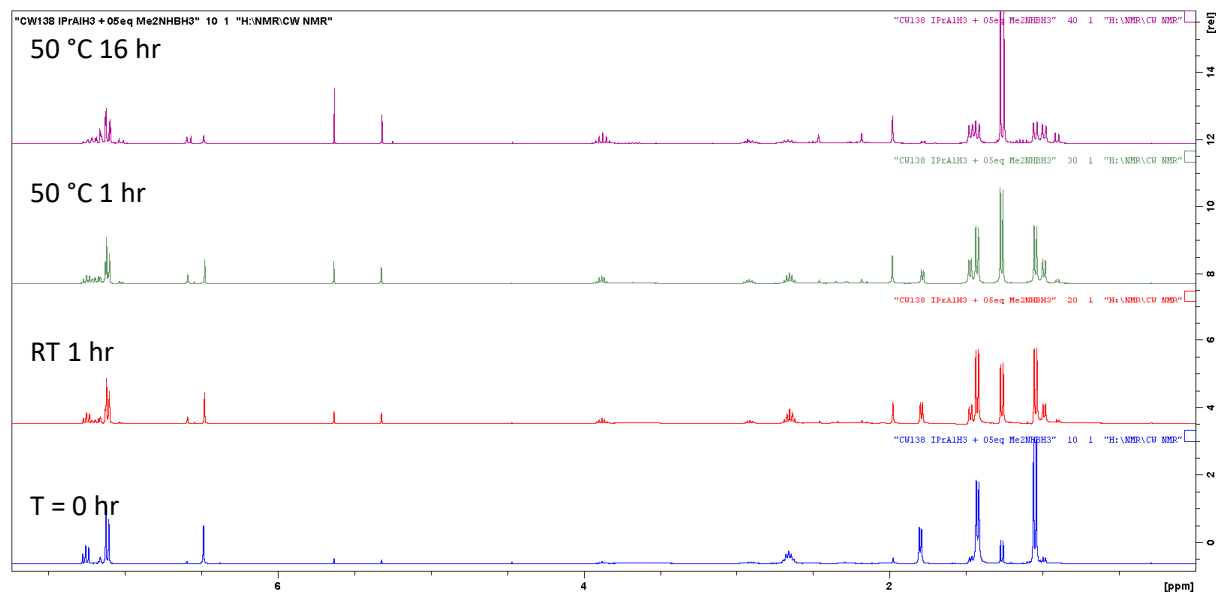


Figure S 19. Stacked  $^1\text{H}$  NMR spectra for stoichiometric reaction between **3** and 0.5 eq. of  $\text{Me}_2\text{NHBH}_3$  in  $\text{C}_6\text{D}_6$ . No reaction occurred at room temperature. At 50 °C o/n resulted in consumption of  $\text{Me}_2\text{NHBH}_3$  with formation of compound **9**.

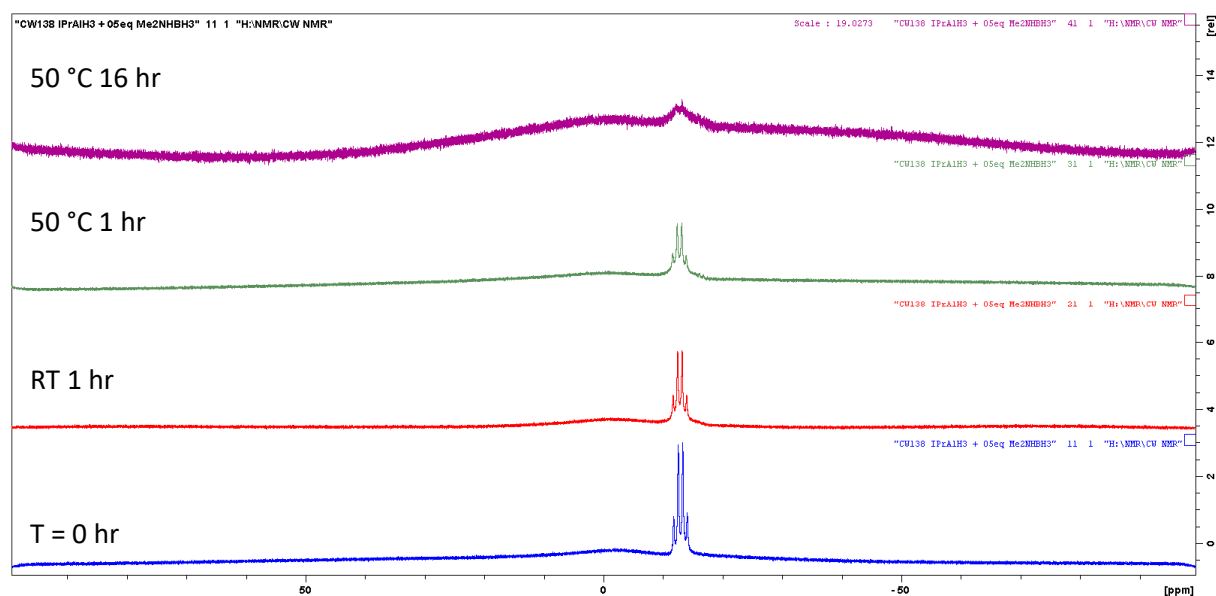


Figure S 20. Stacked  $^{11}\text{B}$  NMR spectra for stoichiometric reaction between **3** and 0.5 eq. of  $\text{Me}_2\text{NHBH}_3$  in  $\text{C}_6\text{D}_6$ . No reaction occurred at room temperature. At 50 °C o/n resulted in consumption of  $\text{Me}_2\text{NHBH}_3$  with formation of compound **9**.

### 3. Data for compounds 8<sup>iPr</sup> and 9

#### 3.1 Compound 8<sup>iPr</sup>

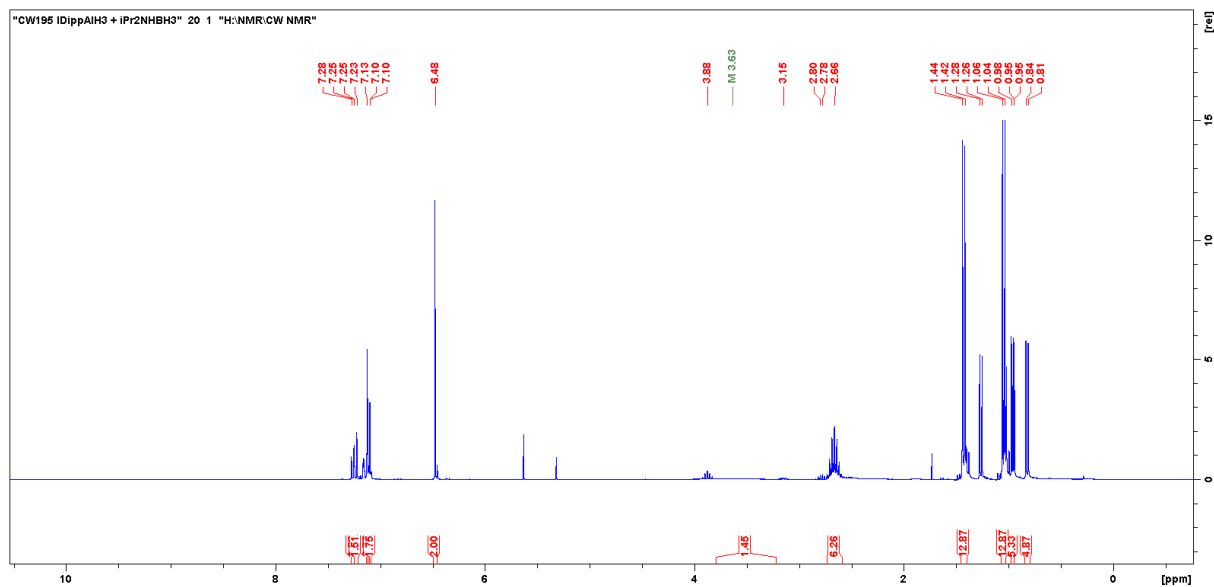


Figure S 21. <sup>1</sup>H NMR spectrum for compound 8<sup>iPr</sup> in C<sub>6</sub>D<sub>6</sub>. Small amount of IDippH<sub>2</sub> present after recrystallisation and additional washes.

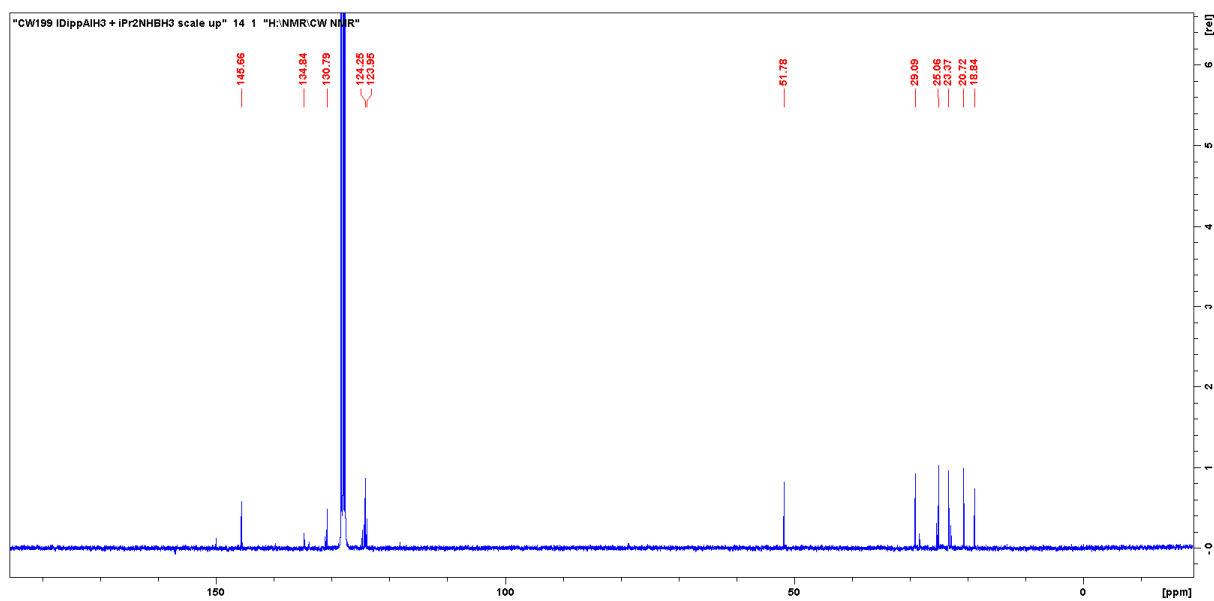


Figure S 22. <sup>13</sup>C NMR spectrum for compound 8<sup>iPr</sup> in C<sub>6</sub>D<sub>6</sub>. Small amount of IDippH<sub>2</sub> present after recrystallisation and additional washes.

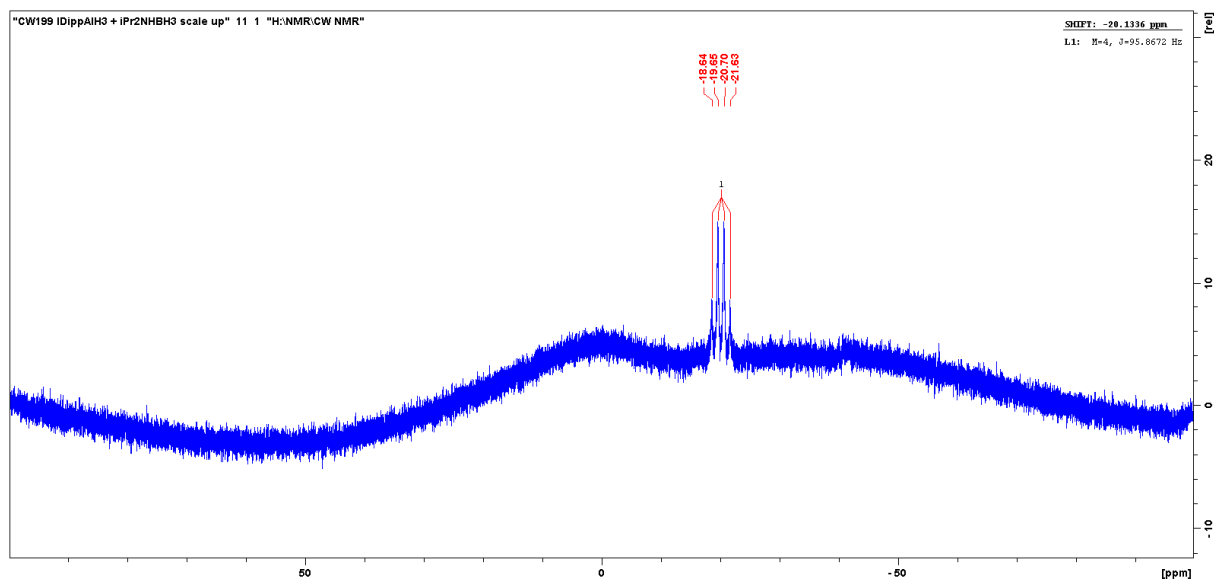


Figure S 23.  $^{11}\text{B}$  NMR spectrum for compound  $\mathbf{8}^{\text{iPr}}$  in  $\text{C}_6\text{D}_6$ . Small amount of IDippH<sub>2</sub> present after recrystallisation and additional washes.

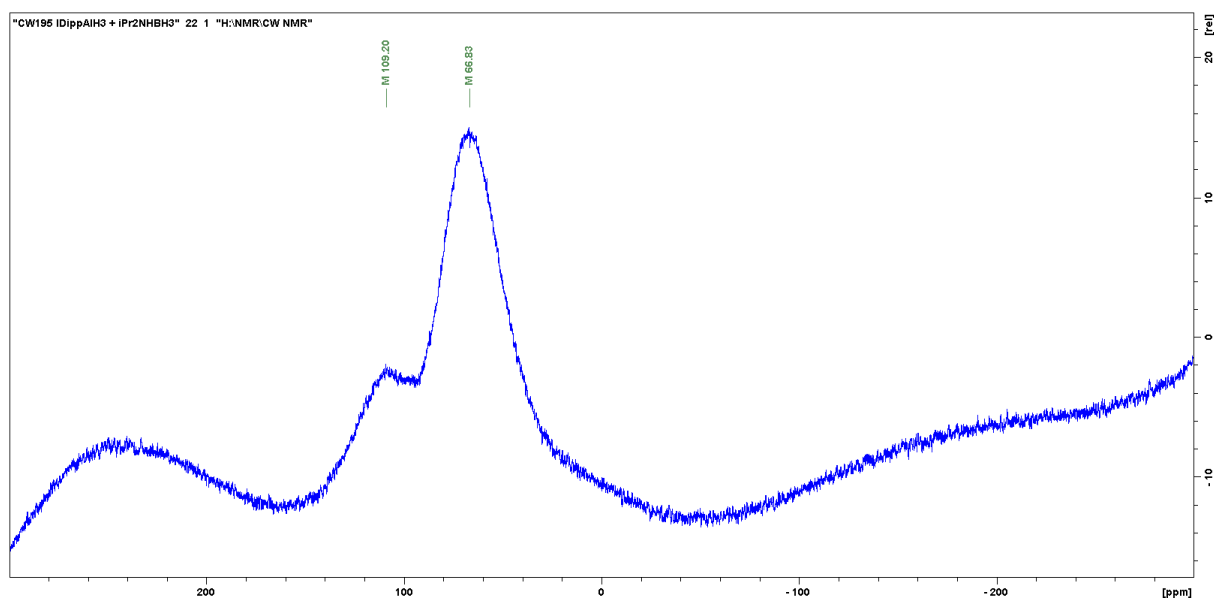


Figure S 24.  $^{27}\text{Al}$  NMR spectrum for compound  $\mathbf{8}^{\text{iPr}}$  in  $\text{C}_6\text{D}_6$ . Small amount of IDippH<sub>2</sub> present after recrystallisation and additional washes.

## 3.2 Compound 9

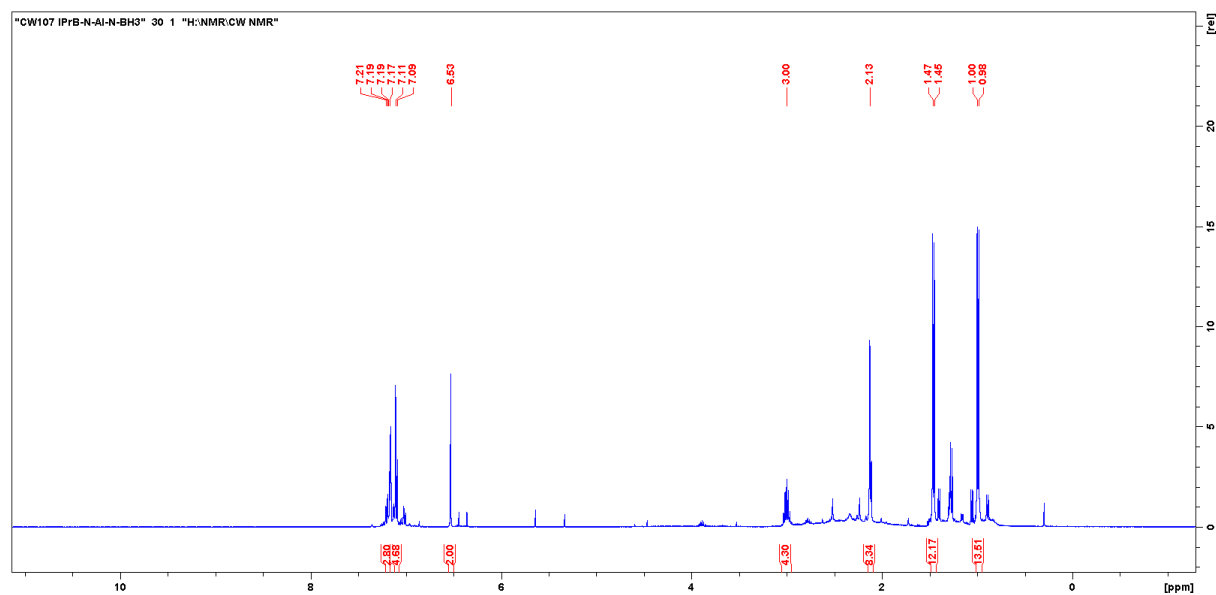


Figure S 25. <sup>1</sup>H NMR spectrum for compound 9 in C<sub>6</sub>D<sub>6</sub>. Small amount of IDippH<sub>2</sub> present after recrystallisation and additional washes.

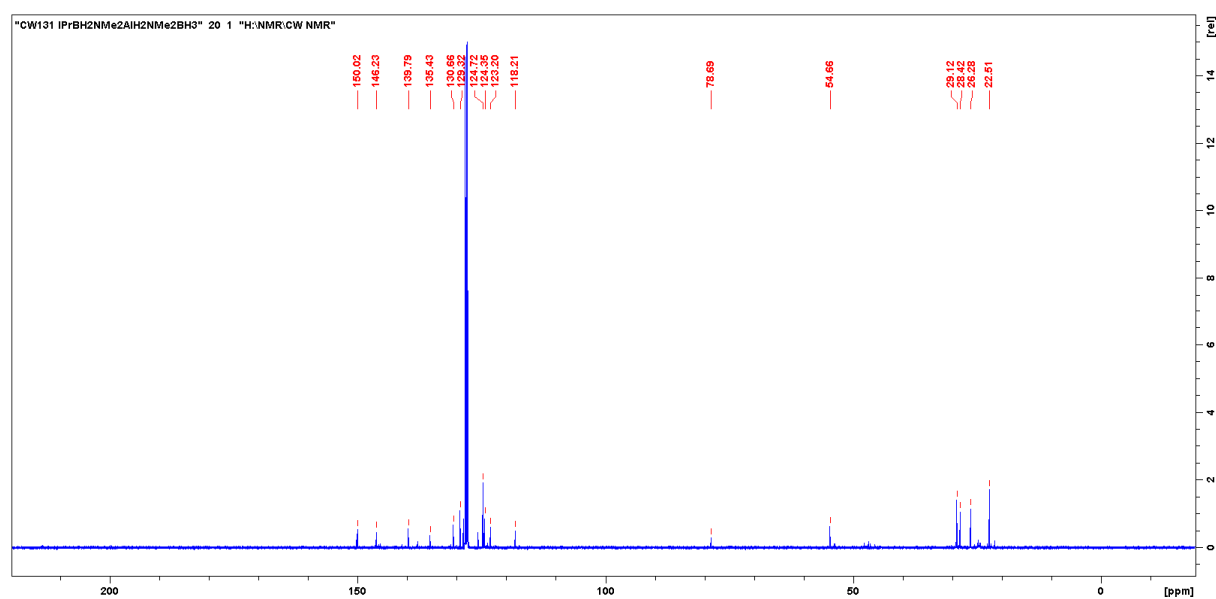


Figure S 26. <sup>13</sup>C{<sup>1</sup>H} NMR spectrum for compound 9 in C<sub>6</sub>D<sub>6</sub>. Small amount of IDippH<sub>2</sub> present after recrystallisation and additional washes.

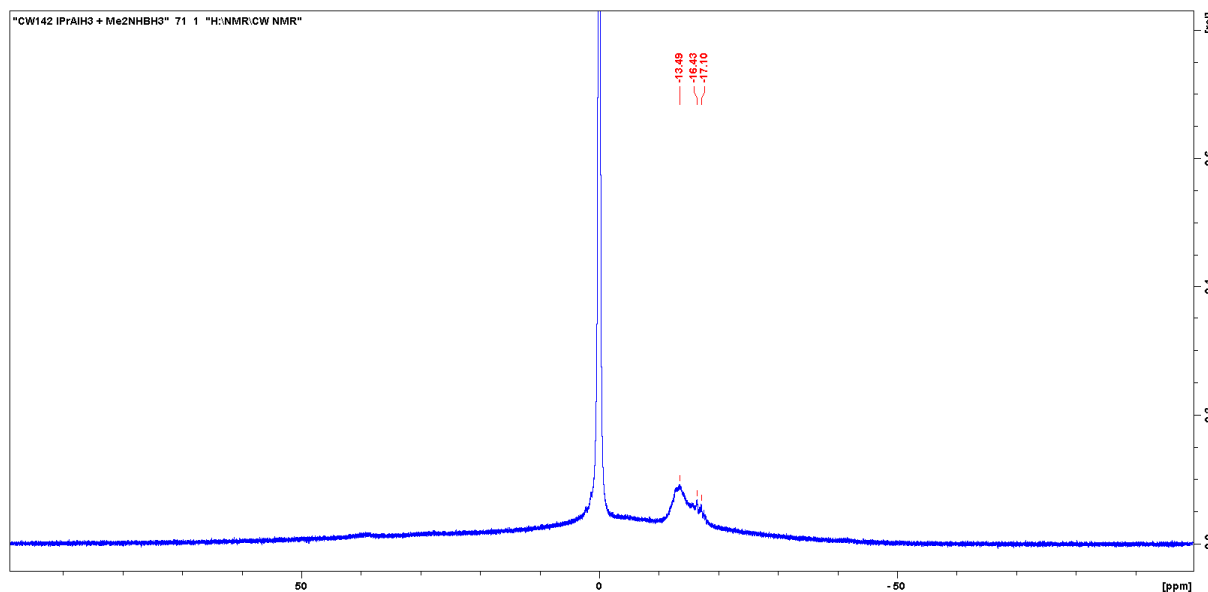


Figure S 27.  $^{11}\text{B}$  NMR spectrum for compound **9** in  $\text{C}_6\text{D}_6$ , with  $\text{BF}_3\cdot\text{OEt}_2$  capillary (0.0 ppm).

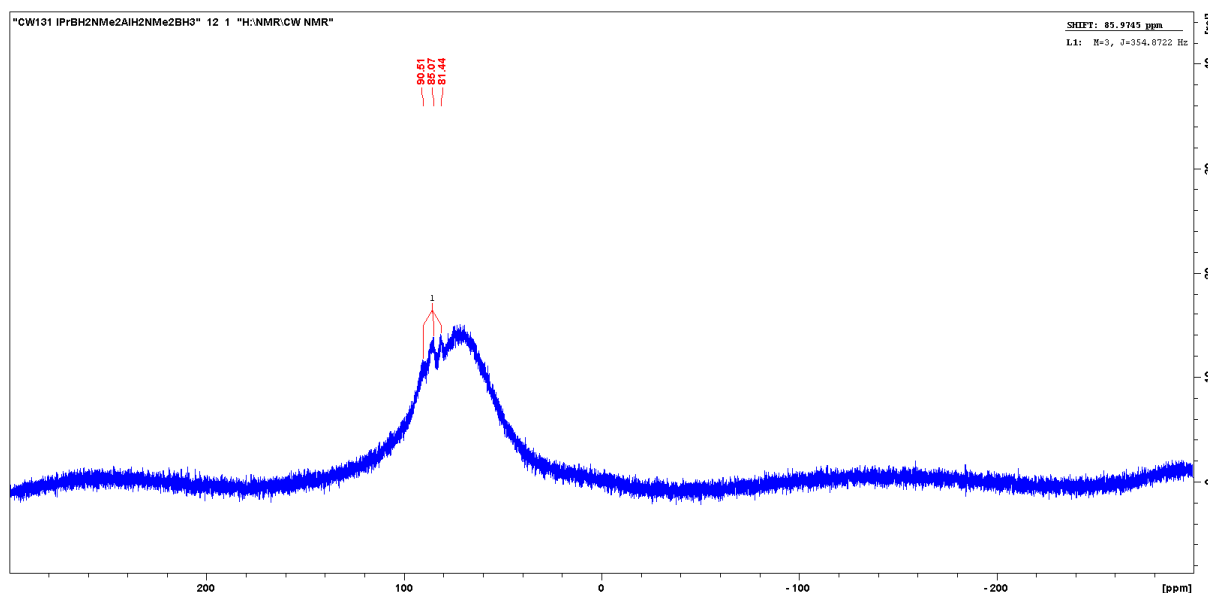


Figure S 28.  $^{27}\text{Al}$  NMR spectrum for compound **9** in  $\text{C}_6\text{D}_6$ .

#### 4. X-ray Data

##### General Information

Single crystal diffraction data were recorded on a Bruker D8 Venture system equipped with a Helios optic monochromator and a Mo TXS rotating anode ( $\lambda = 0.71073 \text{ \AA}$ ). The data collection was performed by using the APEX III software package[S1] on single crystals coated with the perfluorinated ether Fomblin  $\text{\textcircled{R}}$  Y. The single crystal was picked on a micro sampler, transferred to the diffractometer and measured frozen under a stream of 100K nitrogen. A matrix scan was used to determine the initial lattice parameters. Reflections were merged and corrected for Lorenz and polarization effects, scan speed, and background using SAINT.[S2] Absorption corrections, including odd and even ordered spherical harmonics were performed using SADABS.[S2] Space group assignments were based upon systematic absences, E statistics, and successful refinement of the structures. Structures were solved by direct methods with the aid of successive difference Fourier maps, and were refined against all data using the APEX III software in conjunction with SHELXL-2014[S3] and SHELXLE.[S4] H atoms were placed in calculated positions and refined using a riding model, with methylene and aromatic C–H distances of

0.99 and 0.95 Å, respectively, and  $U_{iso}(H) = 1.2 \cdot U_{eq}(C)$ ; except for HB11, HB12, HA1, HA2, HB21, HB22, HB23, which could be located in the difference Fourier maps and were allowed to refine freely. Non-hydrogen atoms were refined with anisotropic displacement parameters. Full-matrix least-squares refinements were carried out by minimizing  $\sum w(F_o^2 - F_c^2)^2$  with the SHELXL weighting scheme.[S5] Neutral atom scattering factors for all atoms and anomalous dispersion corrections for the non-hydrogen atoms were taken from International Tables for Crystallography.[S6] A split layer refinement was used for disordered groups and SIMU and DELU restraints were employed to stabilize the refinement of the layers. The images of the crystal structures were generated by Mercury.[S7] The CCDC number CCDC-1936588 (9) contains the supplementary crystallographic data for the structure. These data can be obtained free of charge from the Cambridge Crystallographic Data Centre via <https://www.ccdc.cam.ac.uk/structures/>.

### X-Ray Crystallographic Table

Table S 2. Crystal data and structural refinement parameters for compound 9.

Compound	9
Molecular formula	C31 H55 Al B2 N4
Molecular weight	532.39
Temperature (K)	100
Wavelength (Å)	0.71073
Space group	P 1 21/c 1
a (Å)	10.135(9)
b (Å)	18.687(14)
c (Å)	19.155(15)
$\alpha$ °	90
$\beta$ °	104.73(2)
$\gamma$ °	90
Volume (Å <sup>3</sup> )	3509(5)
Z	4
D <sub>c</sub> (g cm <sup>-3</sup> )	1.008
$\mu$ (mm <sup>-1</sup> )	0.081
Index ranges	-12<=h<=12, -22<=k<=22, -23<=l<=23
Reflections collected	87849
Unique reflections	6558
Parameter varied	443
Refinement method	Full-matrix least-squares on F <sup>2</sup>
Goodness-of-fit on F <sup>2</sup>	1.059
R <sub>int</sub>	0.1319
R <sub>1</sub>	0.0574
wR <sub>2</sub>	0.1194
Largest diff. peak and hole (eÅ <sup>3</sup> )	0.265 and -0.321

### 4. References

- S1 *APEX suite of crystallographic software*, APEX 3 version 2015.5-2; Bruker AXS Inc.: Madison, Wisconsin, USA, 2015.
- S2 *SAINT*, Version 7.56a and *SADABS* Version 2008/1; Bruker AXS Inc.: Madison, Wisconsin, USA, 2008.
- S3 Sheldrick, G. M. *SHELXL-2014*, University of Göttingen, Göttingen, Germany, 2014.

- S4 Hübschle, C. B.; Sheldrick, G. M.; Dittrich, B. *J. Appl. Cryst.* **2011**, *44*, 1281-1284.
- S5 Sheldrick, G. M. *SHELXL-97*, University of Göttingen, Göttingen, Germany, **1998**.
- S6 Wilson, A. J. C. *International Tables for Crystallography*, Vol. C, Tables 6.1.1.4 (pp. 500-502), 4.2.6.8 (pp. 219-222), and 4.2.4.2 (pp. 193-199); Kluwer Academic Publishers: Dordrecht, The Netherlands, **1992**.
- S7 Macrae, C. F.; Bruno, I. J.; Chisholm, J. A.; Edgington, P. R.; McCabe, P.; Pidcock, E.; Rodriguez-Monge, L.; Taylor, R.; van de Streek, J.; Wood, P. A. *J. Appl. Cryst.* **2008**, *41*, 466-470.